



Derivation and validation of estimation model of rainfall kinetic energy under canopy

Zixi Li¹, Fuqiang Tian¹

¹Department of Hydraulic Engineering, State Key Laboratory of Hydrosience and Engineering, Tsinghua University, Beijing 100084, China

Correspondence to: Fuqiang Tian (tianfq@tsinghua.edu.cn)

Abstract. The interception effect of the canopy on rainfall alters the kinetic energy of the rainfall as it reaches the ground, which is crucial for soil and water conservation, ecosystem stability, and energy transfer within environmental systems. A novel estimation model for the kinetic energy of rainfall under canopy is developed by stratifying the canopy using parameters such as leaf area index and leaf inclination angle, explicitly distinguishing between canopy-dripped and splashed raindrops. The efficacy of the model is subsequently assessed and analyzed through a comprehensive examination of 9 field datasets encompassing LiDAR and raindrop spectrum observations. The simulated under-canopy total kinetic energy, splashing drop kinetic energy, and dripping drop kinetic energy showed average R^2 values of 0.788, 0.613, and 0.768, and average RMSE values of 19.9, 2.2, and 21.1 J/m² h, respectively. Simulations reveal that the canopy exerts a complex influence on the kinetic energy of rainfall beneath it, which may either increase or decrease depending on the physical characteristics of the canopy. The canopy may stabilize the raindrop spectrum and kinetic energy beneath it. Regardless of external variations, these parameters remain constant under an unchanged canopy.

1. Introduction

Canopy interception of rainfall can change both the amount of water amount reaching the ground and the kinetic energy of rainfall, which plays a pivotal role in shaping the hydrological dynamics and ecological integrity of watersheds (Howard, 2022; Momiyama, 2023; Li et al., 2025). The interaction between raindrops and the canopy, encompassing processes such as collision, splashing, and dripping, alters the kinetic energy of rainfall as it reaches the ground. The kinetic energy of rainfall is a crucial parameter with significant implications for soil and water conservation, ecosystem stability, and energy transfer within environmental systems. (Montero-Martínez et al., 2020; Angulo-Martínez et al., 2016).

As the canopy intercepts a portion of the rainfall, it alters the kinetic energy of the rain by modifying the speed and



size of the raindrops that penetrate through (Jeong et al., 2024; Brasil et al., 2022; Nanko et al., 2013; Nanko et al., 2008). The impact of the canopy on the kinetic energy of rainfall, however, is a complex phenomenon, which is influenced by the vegetation type and the physical characteristics such as the leaf area index, leaf orientation, and canopy height (Geißler et al., 2013; Pflug et al., 2021; Tu et al., 2021; Zhang et al., 2023). Research has indicated that larger raindrops are prone to breaking apart into smaller droplets, leading to a decrease in the number of large raindrops and, consequently, a reduction in kinetic energy (Alivio et al., 2023; Senn et al., 2020). Conversely, due to the interception effect, the number of raindrops beneath the canopy is reduced, with a broader distribution range, larger falling droplets, and an increase in kinetic energy (Nanko et al., 2008; Katayama et al., 2024; Zhang et al., 2021).

The method for studying the kinetic energy of rainfall under canopy mainly uses experimental measurement, mainly includes sample cup model, funnel model (Mosley et al., 1983; Van Dijk et al., 2002) and filter paper dyeing method (Yan et al., 2021; Li et al., 2019). While the emerging laser raindrop spectrometer can measure the size and velocity distribution of raindrops more precisely (Fernández-Raga et al., 2010), which facilitates the study of rainfall kinetic energy. Some scholars also use remote sensing methods (Senn et al., 2020; Miralles et al., 2010) to simulate the kinetic energy of rainfall over a large area.

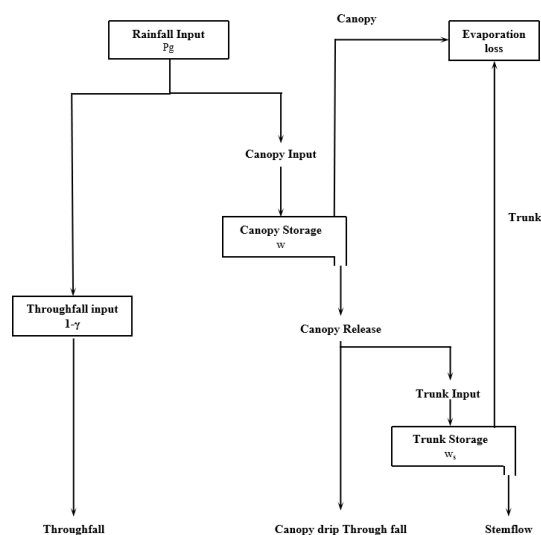
Most existing model for estimating understory kinetic energy are to perform simple function fitting on understory kinetic energy and parameters such as rainfall intensity or canopy height. These methods are highly empirical and have poor adaptability to canopies of different types and properties (Brandt, 1990; Li et al., 2019). Some scholars have considered combining the physical motion processes of raindrops falling and splashing to analyze DSD under the canopy, but a simple and effective simulation method to describe the movement of raindrops in the canopy has not yet been established (Frasson & Krajewski, 2013; Murakami et al., 2021).

Thus, developing an estimation model for kinetic energy under canopy is crucial. This section 2 delves into the canopy interception mechanisms, establishing an understory kinetic energy estimation module. The section 3 validates and analyzes the model simulation performance using 9 field rainfall datasets. The section 4 concludes with a synthesis and outlook on the modeling of rainfall kinetic energy.

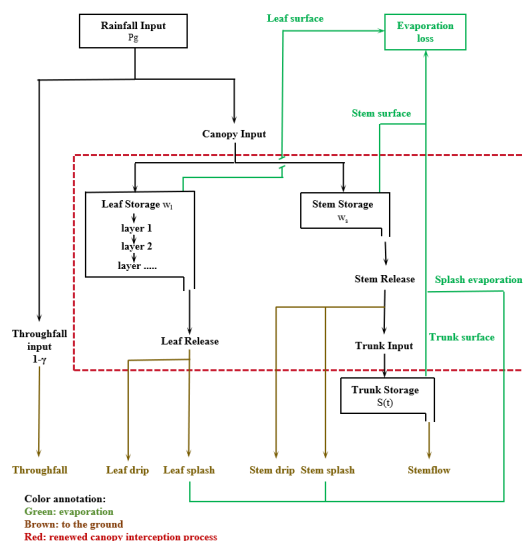
2. Influence of canopy on rainfall energy and model derivation

2.1 Influence of canopy on rainfall energy

The canopy physical function in the interception process involves altering the kinetic energy of raindrops, by



(a) Original canopy interception processes





(b) Refined canopy interception processes

Figure 1. (a) Original canopy interception processes (adapt from Gash and Morton, Valente and Gash); (b) Refined canopy interception processes. The section demarcated by the red dashed lines represents the enhanced portion of the flowchart as compared to the original Rutter model. The primary modifications entail a distinct separation of the interception processes for stems and leaves, acknowledging that the stem area index of certain canopies is substantial, rendering the interception capacity of stems non-negligible (Xiao et al., 2000). Additionally, the updated flowchart incorporates the splash process and the subsequent evaporation of splash droplets from both stems and leaves.

Previous observations and research (Li & Tian, 2025; Frasson & Krajewski, 2013) indicate that the canopy interception flow diagram proposed by Rutter et al. (1997) remains insufficient in capturing the comprehensive physical dynamics and kinetic energy of raindrops. Beyond the canopy drip phenomenon illustrated in Figure 1 (a), raindrops are also subject to breakage and splashing upon collision with the canopy, which plays an important role in kinetic energy change of droplets. This splashing phenomenon is crucial for accurately depicting the canopy interception effect on rainfall (Murakami et al., 2021). Consequently, there is a need to refine the canopy interception process based on the Rutter flow diagram. The revised canopy interception process is depicted in Figure 1 (b).

In Figure 1 (b), for the rainfall intercepted by leaves, the splashing process results in two distinct forms of raindrops: splashed drops and canopy drips. Regarding the interception by stems, the impact of raindrops against the stem leads to some splashing or dripping, while another portion is retained by the stem, eventually contributing to stem flow once the stem is saturated. Given that the velocity of stem flow is significantly slower than that of raindrops falling directly from the sky, some water is retained during this process and the kinetic energy of stem flow is not taken into account. Moreover, evaporation occurs from the splashed drops on both leaves and stems, which, combined with surface evaporation, forms the total rainy season evaporation. Concurrently, water between leaves and stems may interchange during splashing and dripping. However, due to the minimal volume of this water, it is not accounted for in Figure 2 nor in subsequent modeling analyses.

2.2 Model derivation

The core principle of rainfall kinetic energy estimation is to estimate the size and speed of raindrops under the canopy based on the physical and structural properties. Since the shape of a raindrop is not an ideal sphere, the equivalent diameter D (mm) of the raindrop is usually used instead. Therefore, kinetic energy $E(D)$ (J) can be calculated according to the following equation:

$$E(D) = \frac{\pi \rho D^3 v^2}{12} \quad (1)$$



95 where, v is the terminal velocity, ρ is the density of water, which is $1.0 \times 10^{-6} \text{ kg/mm}^3$ under standard conditions. Therefore, the total kinetic energy E_{K_total} (J) is the total kinetic energy calculation can be directly substituted into the simulated raindrop spectrum, such as the gamma function raindrop spectrum, or into the real raindrop spectrum, such as the raindrop spectrum measured by the drop spectrometer:

$$E_{K_total} = \sum_{i=1}^N E(D) \quad (2)$$

Then, calculate the unit area unit rainfall depth kinetic energy E_{Kp} (KE) ($\text{J/m}^2\text{mm}^{-1}$):

$$E_{Kp} = \frac{E_{K_total}}{P \times A} \quad (3)$$

100 where, A is the drop spectrometer observation area (54cm^2), t is the drop spectrometer observation time (60s). The total kinetic energy of rainfall per unit area per unit time E_K ($\text{J/m}^2\text{h}$) is:

$$E_K = \frac{E_{K_total}}{A \times t} = E_{Kp} \times I \quad (4)$$

where, A is the drop spectrometer observation area (54cm^2), t is the drop spectrometer observation time (60s).

Therefore, the corresponding kinetic energy of rainfall under the canopy E_{K_in} ($\text{J/m}^2\text{h}$) is:

$$E_{K_in} = \gamma \cdot E_{K_out} + E_s + E_d \quad (5)$$

where, γ is the canopy density, E_{K_out} is the kinetic energy of rainfall outside the canopy ($\text{J/m}^2\text{h}$), E_s is the splash drop kinetic energy ($\text{J/m}^2\text{h}$), E_d and is the crown drop kinetic energy ($\text{J/m}^2\text{h}$).

For splashing raindrops, the size is about 0.3-1.3mm (see analysis in Section 3.3), and we can assume that the median diameter is about 0.8mm, and the raindrop spectrum is a symmetrical linear distribution with 0.8mm as the maximum value.

For raindrops attached to leaves, crown drops can be divided into dripping raindrops and sliding raindrops according to their movement form. The sizes of the two can be calculated using the following formula (Konrad et al., 2012, Li et al., 2025):

$$s_{max} = l \cdot \frac{(1 + \cos\theta)}{\sqrt{2 + \cos\theta}} \cdot \sqrt{\frac{1 \cdot \sin X}{\pi \cdot \sin\alpha}} \cdot l = \sqrt{\frac{6\sigma}{\rho}} \cdot \sqrt{\frac{1}{g \cdot \sin\alpha + kv^2}} \quad (6)$$

when $\tan\alpha > \frac{2}{\pi} \tan X$, the droplet will slip

$$s_{max} = l \cdot \frac{(1 + \cos\theta)}{\sqrt{2 + \cos\theta}} \cdot \sqrt{\frac{\cos X}{\cos\alpha}}$$

when $\tan\alpha < \frac{2}{\pi} \tan X$, the droplet will drip



where s_{max} (mm) is the maximum radius of the droplet contact surface, θ is the average of the advancing and retreating contact angles on the leaf surface, X is half of the difference between the front and rear contact angles, α is the leaf inclination angle of the canopy, k is a coefficient determined by experiment, which can be selected 0.09 (Li et al., 2025). Therefore, Eqs (6) accounts for the effect of wind load on raindrop size. In subsequent analyses, the term “canopy drip” is used to replace the two physical processes of “slip droplet” and “drip droplet” for the purpose of analysis. The volume of a single droplet is:

$$V = \frac{\pi s^3 (1 - \cos\theta)^2 (2 + \cos\theta)}{3 \sin^3\theta} \quad (7)$$

The mass ratio of the sliding and dripping droplets can be derived based on the leaf inclination angle distribution function.

The droplet velocity can be determined based on Mou J (1983) research:

$$v = \begin{cases} 0.496 \times 10^{\sqrt{28.32+6.524lg0.1d-(lg0.1d)^2-3.665}}, & d < 1.9mm \\ (17.20 - 0.844d)\sqrt{0.1d}, & d > 1.9mm \end{cases} \quad (8)$$

where, d is the raindrop diameter (mm) and v is the final velocity of the raindrop (m/s). When the water drop comes from height h (m), its velocity is (Yao & Chen, 1993):

$$v_{in} = v \times (1 - e^{\frac{-2gh}{v^2}})^{\frac{1}{2}} \quad (9)$$

where h is the falling height (m) and v_{in} is the raindrop velocity inside the canopy (m/s). In the actual canopy, the height h can be taken as the middle height value of the last canopy layer.

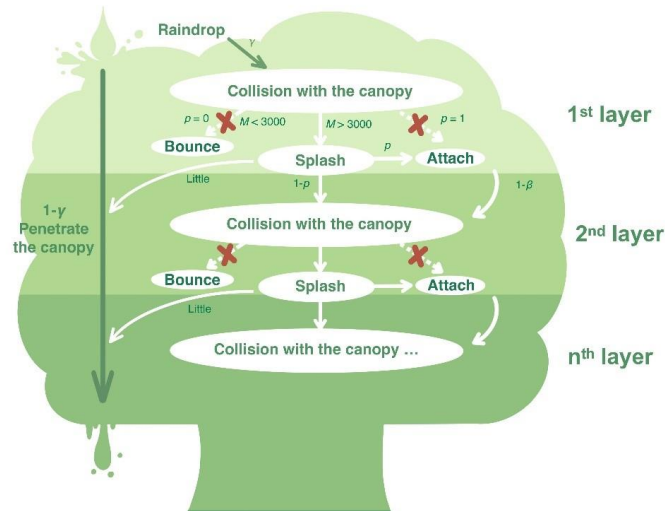


Figure 2. The theoretical canopy interception model based on raindrop microphysical processes raised by Li & Tian (2025)



According to the splash theory and the model of canopy interception microphysical process shown in Figure 2 (Li & Tian, 2025), the ratio of splashing droplets and canopy drip depends on the collision process of the last canopy. if there are $\frac{LAI-G}{\gamma}$ canopy layers, assuming that the saturation level of each canopy layer is consistent and equal to $\frac{w_l}{\gamma}$

130 and considering the splash of stems and leaves at the same time, the amount of water reaching the last canopy I' (mm/h) is:

$$I' = I \times \left[\gamma(1 - p_t) \times (1 - \beta p)^{\frac{LAI-G}{\gamma}-1} + K_l \frac{w_l}{\gamma} + p_t \gamma \right] \quad (10)$$

$$K_l = \gamma [1 - (1 - \beta p)^{\frac{LAI-G}{\gamma}-1}] (1 - p_t)$$

where, γ is FVC, p is pinning proportion coefficient which is defined as the proportion remaining on the leaf after splashing, and then $(1 - p)$ is the proportion of splashed water droplets, β is attachment retention coefficient which is defined as a proportion that remains permanently on the leaf without dripping, $p_t = \frac{SAI}{LAI+SAI}$ is stem flow ratio. In the equations (11), $\left[\gamma(1 - p_t) \times (1 - \beta p)^{\frac{LAI-G}{\gamma}-1} \right]$ describes the proportion that is not intercepted by the leaves, $\left[K_l \frac{w_l}{\gamma} \right]$ represents the proportion of leaves that penetrate the canopy due to saturation, and $[p_t \gamma]$ describes the proportion of raindrops colliding with the stem (assuming that the stem only has one layer). The canopy interception volume w_l is calculated based on the simplified model form raised by Li & Tian (2025).

Therefore, the proportion of splash drops is:

$$k_s = (1 - p) \times \left[\gamma(1 - p_t) \times (1 - \beta p)^{\frac{LAI-G}{\gamma}-1} + K_l \frac{w_l}{\gamma} + p_t \gamma \right] \quad (11)$$

140 the proportion of canopy drip is:

$$k_a = p \times \left[(1 - \beta) \gamma (1 - p_t) \times (1 - \beta p)^{\frac{LAI-G}{\gamma}-1} + K_l \frac{w_l}{\gamma} + \gamma p_t D_d \times \frac{w_s}{S} \right] \quad (12)$$

where, D_d is defined as the proportion of canopy drip in the stem flow. The splash droplet mass m_s and canopy drip mass m_a per unit area per unit time (kg/m²h) are:

$$m_s = \rho \times I \times k_s$$

$$m_a = \rho \times I \times k_a \quad (13)$$

At last, E_{K_in} (J/m²h) is:

$$E_{K_in} = \gamma \cdot E_{K_out} + \frac{1}{2} \int dm_s v_s^2 + \frac{1}{2} \int dm_a v_a^2 \quad (14)$$

In summary, the simulation calculation steps of the kinetic energy under canopy are as follows: first calculate the crown drop size distribution according to eq (7), then calculate the landing speed of raindrops of different sizes



according to eqs (9), then calculate the splash drop and crown drop mass per unit area per unit time according to eqs (10-13), and finally calculate the kinetic energy of raindrops per unit area per unit time under the canopy according to eq (14) (J/m²h).

The influence of wind load and rainfall intensity will cause changes in the canopy interception capacity. After the rainfall, droplets will still drip due to leaf vibration, generating dripping kinetic energy, which is generally manifested as the hysteresis effect of the understory kinetic energy. In order to better simulate the real-time rainfall kinetic energy intensity, this model allocates the changes in the canopy interception capacity caused by factors such as wind load to a total of 15 minutes after this rainfall period in a ratio of 0.7, 0.2, and 0.1 in units of 5 minutes to describe the hysteresis effect of the understory kinetic energy.

The estimation model of rainfall kinetic energy under canopy can be summarized as Table 1.

Table 1. Summary of the model of rainfall kinetic energy under canopy

Model variables	Model form
Leaf interception (mm)	$\frac{IK_l Y}{IK_l + e_{pl}} \left[1 - e^{-\left(\frac{IK_l + e_{pl}}{Y}\right)t} \right]$ $K_l = \gamma [1 - (1 - \beta p)^{\frac{LAI \cdot G}{Y}}] (1 - p_t)$
Stem interception (mm)	$\frac{IK_s S}{IK_s + e_{ps}} \left[1 - e^{-\left(\frac{IK_s + e_{ps}}{S}\right)t} \right]$ $K_s = \gamma \times p_t$
Stem dripping (mm/h)	$I \times K_s \times D_d \times \frac{W_s}{S}$
Stem splashing (mm/h)	$I p_t \gamma \times (1 - p)$
Leaf dripping (mm/h)	$I \times p \times \left[(1 - \beta) \gamma (1 - p_t) \times (1 - \beta p)^{\frac{LAI \cdot G}{Y} - 1} + K_l \frac{W_l}{Y} \right]$
Leaf splashing (mm/h)	$I \times (1 - p) \times \left[\gamma (1 - p_t) \times (1 - \beta p)^{\frac{LAI \cdot G}{Y} - 1} + K_l \frac{W_l}{Y} \right]$
Raindrop velocity under canopy (m/s)	$v = \begin{cases} 0.496 \times 10^{\sqrt{28.32 + 6.524 \lg 0.1d - (\lg 0.1d)^2 - 3.665}}, & d < 1.9mm \\ (17.20 - 0.844d)\sqrt{d}, & d > 1.9mm \end{cases}$ $v_{in} = v \times (1 - e^{-\frac{2gh}{v^2}})^{\frac{1}{2}}$
Penetration Energy (J/m ² h)	$\gamma \cdot E_{K_out}$
Splash kinetic energy (J/m ² h)	$\frac{1}{2} \int dm_s v_s^2$ $m_s = \rho \times k_s$ $k_s = (1 - p) \times \left[\gamma (1 - p_t) \times (1 - \beta p)^{\frac{LAI \cdot G}{Y} - 1} + K_l \frac{W_l}{Y} + p_t \gamma \right]$



Canopy drip kinetic energy (J/m ² h)	$\frac{1}{2} \int dm_a v_a^2$ $m_a = \rho \times k_a$ $k_a = p \times \left[(1 - \beta)\gamma(1 - p_t) \times (1 - \beta p)^{\frac{LAI \cdot G}{\gamma} - 1} + K_l \frac{w_l}{Y} + \gamma p_t D_d \times \frac{w_s}{S} \right]$
--	--

Note: γ is the fractional vegetation cover (FVC), w_s is the stem interception volume (mm), w_l is the leaf interception volume (mm), I is the rainfall intensity (mm/h), Y is the leaf interception capacity (mm), S is the stem interception capacity (mm), e_{ps} is the stem evaporation intensity (mm/h), e_{pl} is the leaf evaporation intensity (mm/h), d is the raindrop diameter (mm), t is the rainfall duration (h), K_s is the stem interception coefficient, K_l is the leaf interception coefficient, p_t is stem area proportion, p is the splash pinning proportion coefficient, β is the attachment retention coefficient, D_d is the proportion of canopy drip in the stem flow, SAI is the stem area index, LAI is the leaf area index, G is the leaf area projection ratio, v is final velocity of the raindrop, v_{in} is the raindrop velocity inside the canopy (m/s), $E_{K,out}$ is the rainfall kinetic energy per unit area per unit time outside the canopy, $E_{K,in}$ is the kinetic energy per unit area per unit time inside the canopy, ρ is the density of water (kg/m³), k_s is the splash intensity (mm/h), k_a is the canopy dripping intensity (mm/h), m_s is the splash mass per unit area per unit time, m_a is the dripping mass per unit area per unit time (kg/m²s), v_s is the splash droplet velocity (m/s), v_a is the dripping droplet velocity (m/s).

3. Experimental validation and analysis

3.1 Canopy experimental method

To assess the model simulation efficacy, this research conducted observations of 9 rainfall events on *Aesculus chinensis* Bunge within the Tsinghua University campus. For raindrop spectrum observations, two OTT Parsivel² laser spectrometer were utilized, capable of dividing particle size and velocity into 32 bins, totaling 1024 combinations, with a size range of 0.0625 mm to 24.5 mm and a velocity range of 0.05 to 20.8 m/s. One of the laser spectrometers was situated under a *Aesculus chinensis* Bunge (116.3°E, 40.0°N), while the other was mounted on the roof of Tsinghua University sediment laboratory, approximately 150 meters away, assumes similar rainfall characteristics.

As an effective means of observation, LiDAR has been widely used in the observation and analysis of vegetation structural parameters in recent years (Wang et al., 2023; Mostafa et al., 2022). In this study, Rigel VZ600i ground-based radar was used to observe and extract canopy parameters. Its ranging accuracy was 5 mm within 100 m and the scanning angle accuracy was 0.0028°. The FVC (Fraction of Vegetation Cover) is obtained from the voxel void statistics in the vertical direction. The leaf area density was calculated using the VCP algorithm based on contact frequency (Chen et al., 2024; Hosoi & Omasa, 2006), and then the LAI was obtained by integration along the vertical direction. The leaf inclination angle distribution was calculated using the principal component analysis method based on the leaf normal vector (Maćkiewicz & Ratajczak, 1993). The stem area index and stem inclination angle parameters were extracted based on the branch reconstruction algorithm (Du et al., 2019), and the leaf area projection



ratio G can be calculated according to the leaf inclination distribution. The basic parameters of *Aesculus chinensis* Bunge were measured as follows: LAI is 10.67, SAI is 1.26, FVC is 0.976, the last canopy layer height h_l is 4.85m, and G is 0.59. The model was validated and analyzed using data from nine rainfall events observed in 2024. The observation dates, accumulated rainfall, mean wind speed, and mean rainfall intensity are presented in Table 3. The model parameters under field experimental conditions need to be determined, as shown in Table 2.

Table 2. Parameters of estimation model of rainfall kinetic energy under canopy

Type	Symbol	Value	Physical meaning	Unit
Rainfall	R	Measured	Rainfall intensity	mm/h
	d_r	Calculated by rainfall intensity-radius relationship or measured	Raindrop median diameter	mm
Canopy	LAD	Measured	Leaf inclination distribution	°
	G	Calculated by LAD	Leaf area projection coefficient	—
	γ	Measured	FVC	—
	LAI	Measured	Leaf area index	—
	SAI	Measured	Stem area index	—
	h_l	Measured	The last canopy layer height	m
	w	Calculated by interception model (Li & Tian, 2025; Li et al., 2025)	Canopy interception amount	mm

3.2 Validation and Rainfall kinetic analysis

This section evaluates and analyzes the performance of the understory kinetic energy estimation model by integrating raindrop spectrum observation data of *Aesculus chinensis* Bunge on 9 field rainfall events shown in Table 3.

Table 3. R^2 and RMSE Performance Metrics for Canopy Rainfall Kinetic Energy Partitioning

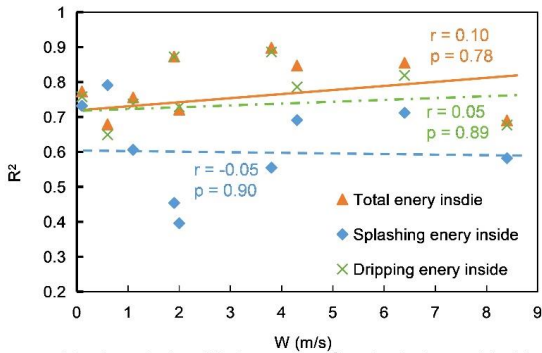
Observation time	Accumulat-ed rainfall (mm)	Wind speed (m/s)	Rainfall intesnity (mm/h)	Total kinetic energy under canopy		Splashing drop kinetic energy under canopy		Driping drop kinetic energy under canopy	
				R^2	RMSE (J/m ² h)	R^2	RMSE (J/m ² h)	R^2	RMSE (J/m ² h)
2024.6.25	5.72	0.6	5.42	0.679	26.1	0.791	2.0	0.649	30.2
2024.6.29	5.28	1.1	3.17	0.756	14.5	0.606	1.3	0.737	16.0
2024.7.1	8.51	0.1	6.96	0.773	35.4	0.732	4.4	0.758	36.6
2024.7.19	7.45	8.4	7.65	0.690	46.9	0.582	5.9	0.677	49.4
2024.7.25	7.05	3.8	2.01	0.898	4.0	0.555	0.6	0.886	4.1
2024.7.29	4.73	2.0	2.03	0.721	7.9	0.396	0.8	0.729	7.8
2024.8.20	4.63	4.3	5.56	0.847	22.5	0.691	3.6	0.786	24.7
2024.8.25	4.94	6.4	3.71	0.855	16.8	0.712	1.1	0.819	16.2



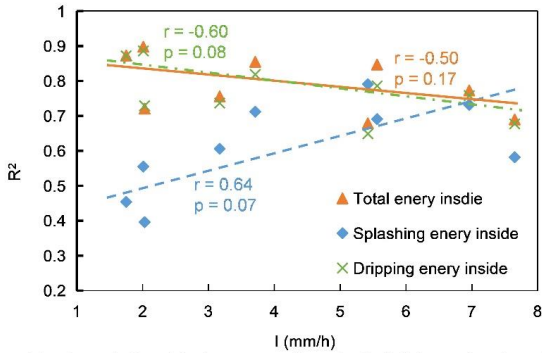
2024.8.26	6.71	1.9	1.75	0.873	5.1	0.454	0.4	0.872	5.0
Average				0.788	19.9	0.613	2.2	0.768	21.1

Table 3 presents the R^2 and RMSE metrics for the simulated under-canopy total kinetic energy, splashing drop kinetic energy, and dripping drop kinetic energy (J/m^2h) derived from these nine rainfall events. The average R^2 values were 0.788, 0.613, and 0.768, and the average RMSE values were 19.9, 2.2, and 21.1 J/m^2h , respectively.

Overall, the simulation accuracy for all three components is satisfactory. The simulation of under-canopy dripping kinetic energy demonstrated higher accuracy than that of splashing kinetic energy, likely due to the greater complexity and higher uncertainty associated with the splashing phenomenon which is shown in Figure 4 and 5.



(a) The relationship between R^2 and wind speed (m/s)



(b) The relationship between R^2 and rainfall intensity (mm/h)

Figure 3. Correlation Analysis Between Model Metric R^2 and Influencing Factors: (a) Wind Speed, (b) Rainfall Intensity.

Since the RMSE metric is influenced by the total kinetic energy outside the canopy, the R^2 metric was adopted for the correlation analysis of influencing factors, as shown in Figure 3. Figure 3 indicates that wind load has no significant effect on model performance, with p-values consistently above 0.7. This likely occurs because the



estimation of under-canopy raindrop size distribution accounts for wind load effects (see Eqs 6 in Section 2.2),
 maintaining relatively stable model performance across varying wind speeds. As mean rainfall intensity increases,
 the performance for total kinetic energy and dripping kinetic energy shows a declining trend, while splashing kinetic
 energy exhibits an increasing trend. Although none reached statistical significance ($p < 0.05$), the p-values around
 0.08 indicate noticeable trends. This may be attributed to: (1) splashing being less pronounced at low rainfall
 intensities, leading to biased splashing energy estimates; and (2) significant leaf vibration induced by high rainfall
 intensities, which is not currently considered in the model, resulting in slightly diminished performance with
 increasing rainfall intensity.

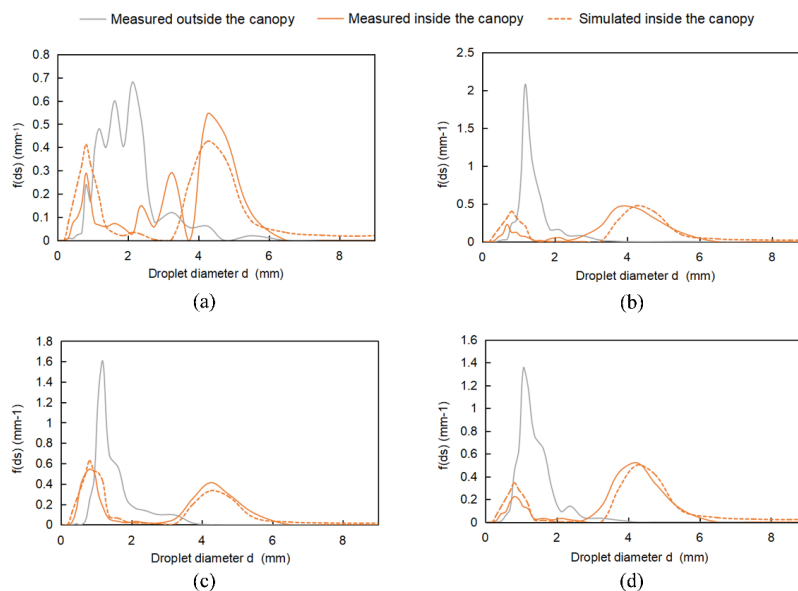
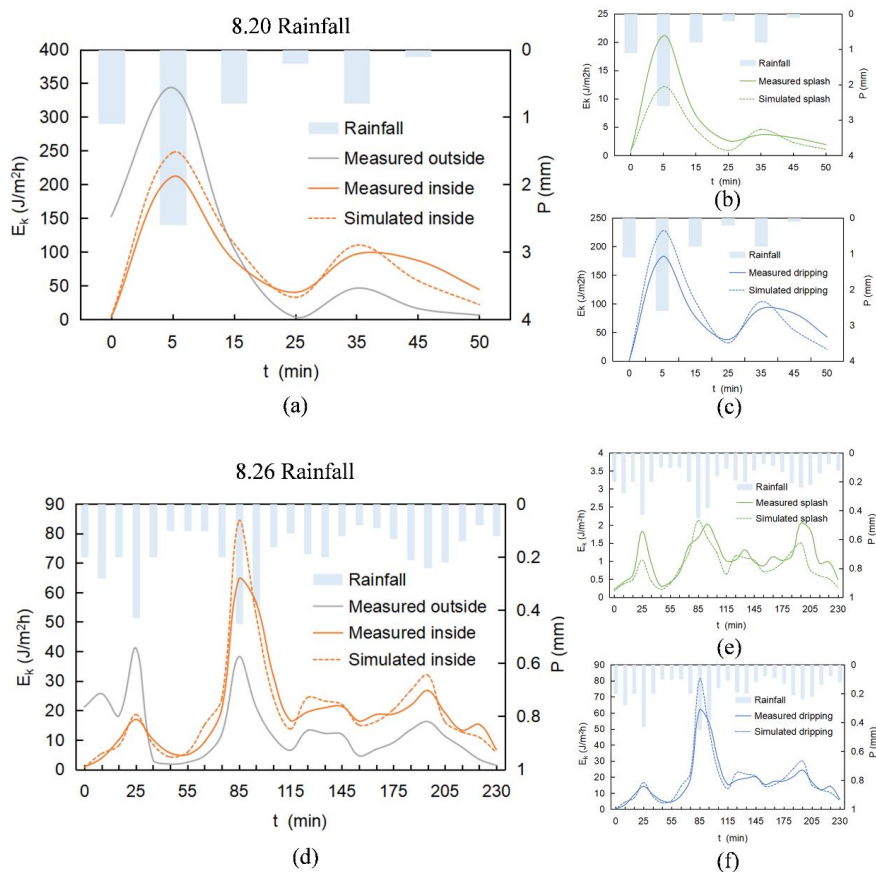


Figure 4. Comparison of raindrop spectra outside the canopy and inside the canopy during two rainfall events (a) Raindrop spectrum of 0-10 min rainfall on 8.20 (b) Raindrop spectrum of 30-40 min rainfall on 8.20 (c) Raindrop spectrum of 0-10 min rainfall on 8.26 (d) Raindrop spectrum of 150-160 min rainfall on 8.26.

Taken rainfall events on 8.20 and 8.26 as examples, the raindrop spectrum data collected beneath the canopy reveals a trend of relative consistency between the measured and simulated raindrop sizes, which is shown in Figure 4. Raindrops smaller than 1.5 mm, which are primarily responsible for splashing (Levia et al., 2017), constitute approximately 10%-30% of the mass ratio. The proportion of measured raindrops within the splashing size range is lower than that of the simulation, which may be attributed to the fact that not all splashed drops fall within the 0.3-1.3 mm bracket and larger splashes are also present. Over time, as canopy saturation increases, the relative frequency



of splashing drops in both measured and simulated data decreases, while the proportion of dripping raindrops rises. This behavior is consistent across both datasets and aligns with the physical expectation that higher canopy saturation leads to greater canopy dripping intensity. The measured raindrop spectrum shows a smaller size distribution in the dripping range compared to the simulation results. This discrepancy could be due to leaf vibrations causing the falling raindrops to be smaller than the values calculated, thereby resulting in a lower simulated kinetic energy. Figure 4 also suggests that the canopy exerts an aggregating effect on the kinetic energy of rainfall, indicating that for canopies with similar physical structures, the raindrop spectrum and distribution under the canopy remain relatively stable regardless of variations in the external raindrop spectrum. Based on the analysis in Section 2.2, this phenomenon occurs because the sub-canopy raindrop spectrum (excluding direct throughfall) is primarily governed by canopy physical parameters such as leaf area index, leaf inclination angle, and leaf contact angle, through raindrop interactions including splashing, dripping, and coalescence within the canopy.



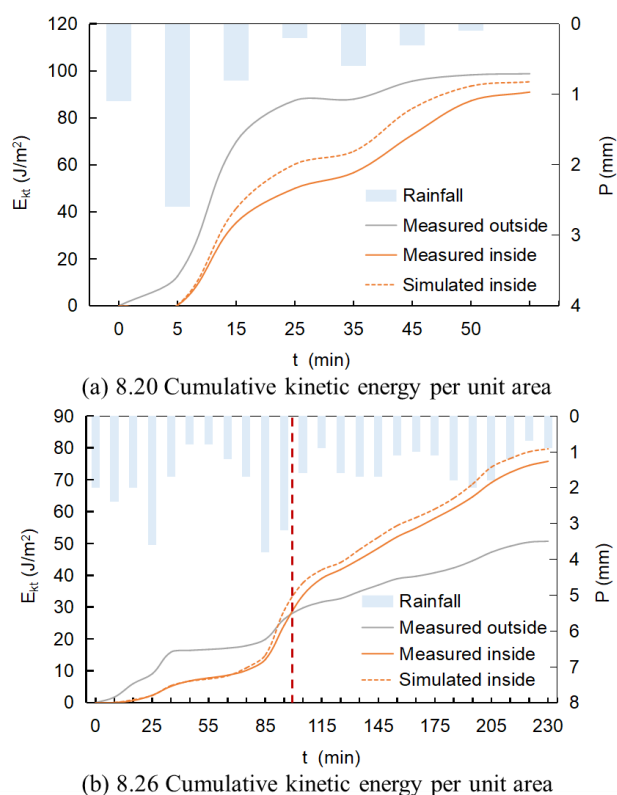


240 **Figure 5. Comparison of kinetic energy of rainfall outside the canopy during two rainfall events (a) 8.20 total kinetic energy of rainfall (b) 8.20 kinetic energy of splashing drops under the canopy (c) 8.20 kinetic energy of dripping drops under the canopy (d) 8.26 total kinetic energy of rainfall (e) 8.26 kinetic energy of splashing drops under the canopy (f) 8.26 kinetic energy of dripping drops under the canopy.**

245 Figure 5 demonstrates decreased kinetic energy under canopy compared to open areas during rainfall, as canopy interception reduces rainwater reaching the ground. As the canopy nears saturation, sub-canopy kinetic energy increases significantly due to enhanced formation of large canopy drips (>3.5 mm radius). The comparison between measured and simulated kinetic energy shows higher peak values in the simulation, even after accounting for hysteresis effects, which potentially results from smaller measured drip sizes in the raindrop spectrum (Figure 4)

250 relative to simulations, which may cause kinetic energy overestimation.

The complexity of the splash phenomenon, including the presence of larger splash drops not accounted for in the simulation symmetrical linear distribution assumption with a maximum diameter of 0.8 mm, may explain the discrepancy. However, since splash droplet kinetic energy constitutes a small fraction of the total kinetic energy (about 3%-10%), its impact on the overall simulation is minimal.



255

Figure 6. Cumulative kinetic energy per unit area. (a) 8.20 Rainfall, (b) 8.26 Rainfall

Figure 6 compares measured and simulated cumulative kinetic energy per unit area in open versus sub-canopy conditions during two rainfall events. The simulations demonstrate high accuracy with R^2 values of 0.90 and 0.93. Initially, sub-canopy energy remains lower than open rainfall due to canopy interception. As the canopy approaches saturation, increased canopy dripping drives significant energy escalation beneath the canopy. Specifically, for the 20 August event, persistently lower sub-canopy energy results from high interception ratio ($\sim 19\%$). In contrast, during the 26 August event, sub-canopy energy surpasses open rainfall at $t \approx 100$ min, ultimately reaching nearly twice the open-environment value as interception efficiency declines to 13%.

Consequently, assessing the canopy impact on rainfall kinetic energy requires a comprehensive analysis of canopy leaf inclination, contact angle, branch height, and the external raindrop spectrum to determine whether the kinetic energy beneath the canopy is greater or less than that outside. Smaller branch heights and larger leaf inclination angles may result in fewer and slower dripping raindrops, potentially leading to lower kinetic energy under the canopy. This variability likely explains the disparate experimental results and viewpoints among scholars regarding the canopy

265



impact on rainfall kinetic energy.

270 4. Summary

Based on the research of [Li & Tian \(2025\)](#), this study established the new rainfall kinetic energy under canopy estimation model, combined with high-precision LiDAR data to obtain canopy physical parameters, and used 9 field rainfall experimental observations to verify the model simulation results. The analysis led to the following conclusions:

- 275 1. The introduction of splash and canopy drip mechanisms into canopy interception modeling, enhanced by LiDAR-derived structural parameters, enables simulation of sub-canopy raindrop spectra and kinetic energy. This approach shows preliminary potential for soil erosion studies, though further validation with expanded datasets is required given current limitations to 9 rainfall events.
2. The influence of the canopy on the kinetic energy of rainfall is more complicated, which can be simulated by this
- 280 model. The increase or decrease of the kinetic energy under the canopy mainly depends on the physical properties of the canopy such as interception intensity, splash retention coefficient and leaf inclination distribution.
3. The canopy may have an aggregation effect on the raindrop spectrum and rainfall kinetic energy. No matter how the raindrop spectrum outside the canopy changes, the raindrop spectrum and raindrop kinetic energy under the canopy are constant when the physical properties of canopy remain unchanged.
- 285 This study is limited to analyses from 9 rainfall events on a single broadleaf species. Further validation across more tree species and rainfall events is required to extend the model's applicability.

Data Available Statement

The data used in the study, such as raindrop spectrum observations, data of rainfall kinetic energy, and model running python code are available at Zenodo ([Li, 2025](#)).

290 Acknowledgments

This study has been supported by the National Natural Science Foundation of China (U2442201 & 523B1006), and the National Key Research and Development Program of China (2022YFC3002900).



References

- Alivio, M. B., Bezak, N., and Mikoš, M.: The size distribution metrics and kinetic energy of raindrops above and
 295 below an isolated tree canopy in urban environment, *Urban For. Urban Greening*, 85, 127971, doi:10.1016/j.ufug.2023.127971, 2023.
- Brasil, J. B., Andrade, E. M. D., Araújo de Queiroz Palácio, H., Fernández-Raga, M., Carvalho Ribeiro Filho, J.,
 Medeiros, P. H. A., and Guerreiro, M. S.: Canopy effects on rainfall partition and throughfall drop size
 distribution in a tropical dry forest, *ATMOSPHERE-BASEL*, 13, 1126, doi:10.3390/atmos13071126, 2022.
- 300 Chen, C., Jia, Y., Zhang, J., Yang, L., Wang, Y., and Kang, F.: Development of a 3D point cloud reconstruction-
 based apple canopy liquid sedimentation model, *J. Cleaner Prod.*, 451, 142038, doi:10.1016/j.jclepro.2024.142038, 2024.
- de Moraes Frasson, R. P., and Krajewski, W. F.: Rainfall interception by maize canopy: Development and
 application of a process-based model, *J. Hydrol.*, 489, 246–255, doi:10.1016/j.jhydrol.2013.03.019, 2013.
- 305 Du, S., Lindenberg, R., Ledoux, H., Stoter, J., and Nan, L.: AdTree: Accurate, detailed, and automatic modelling
 of laser-scanned trees, *Remote Sens.*, 11, 2074, doi:10.3390/rs11182074, 2019.
- Gash, J. H. C., and Morton, A. J.: An application of the Rutter model to the estimation of the interception loss from
 Thetford forest, *J. Hydrol.*, 38, 49–58, doi:10.1016/0022-1694(78)90131-2, 1978.
- Geißler, C., Nadrowski, K., Kühn, P., Baruffol, M., and Bruelheide, H.: Kinetic Energy of Throughfall in Subtropical
 310 Forests of SE China – Effects of Tree Canopy Structure, Functional Traits, and Biodiversity, *PLoS ONE*, 8,
 e49618, doi:10.1371/journal.pone.0049618, 2013.
- Fernández-Raga, M., Fraile, R., Keizer, J. J., Teijeiro, M. E. V., Castro, A., Palencia, C., and Marques, R. L. D. C.:
 The kinetic energy of rain measured with an optical disdrometer: An application to splash erosion, *Atmos. Res.*,
 96, 225–240, doi:10.1016/j.atmosres.2009.07.013, 2010.
- 315 Hosoi, F., and Omasa, K.: Voxel-based 3-D modeling of individual trees for estimating leaf area density using high-
 resolution portable scanning lidar, *IEEE Trans. Geosci. Remote Sens.*, 44, 3610–3618,
 doi:10.1109/TGRS.2006.881743, 2006.
- Howard, M., Hathaway, J. M., Tirpak, R. A., Lisenbee, W. A., and Sims, S.: Quantifying urban tree canopy
 interception in the southeastern United States, *Urban For. Urban Greening*, 77, 127741,
 320 doi:10.1016/j.ufug.2022.127741, 2022.
- Katayama, A., Nanko, K., Jeong, S., Kume, T., Shinohara, Y., and Seitz, S.: Concentrated impacts by tree canopy
 drips: Hotspots of soil erosion in forests, *Earth Surf. Dyn. Discuss.*, 2023, doi:10.5194/esurf-11-1275-2023 1–
 12, 2023.
- Konrad, W., Ebner, M., Traiser, C., and Roth-Nebelsick, A.: Leaf Surface Wettability and Implications for Drop
 325 Shedding and Evaporation from Forest Canopies, *Pure Appl. Geophys.*, 169, 835–845, doi:10.1007/s00024-
 011-0330-2, 2012.
- Levia, D. F., Carlyle-Moses, D., and Tanaka, T.: Forest hydrology and biogeochemistry: synthesis of past research
 and future directions, *Springer Sci. Bus. Media*, 216, 2011.



- Li, G., Wan, L., Cui, M., Wu, B., and Zhou, J.: Influence of canopy interception and rainfall kinetic energy on soil erosion under forests, *FORESTS*, 10, 509, doi:10.3390/f10060509, 2019.
- Li, Z.: The open data of "Derivation and validation of estimation model of rainfall kinetic energy under canopy", Zenodo, doi.org/10.5281/zenodo.15472339, 2025.
- Li, Z., and Tian, F.: Derivation and validation of a theoretical canopy interception model based on raindrop microphysical processes, *Water Resour. Res.*, 61, e2024WR038296, doi:10.1029/2024WR038296, 2025.
- Li, Z., Tian, F., Wang, D., and Peng, Z.: A stochastic simulation method for estimating vegetation interception capacity based on mechanical-geometric analysis, *Water Resour. Res.*, 61, e2025WR040267, doi:10.1029/2025WR040267, 2025.
- Maćkiewicz, A., and Ratajczak, W.: Principal components analysis (PCA), *Comput. Geosci.*, 19, 303–342, 1993.
- Miralles, D. G., Gash, J. H., Holmes, T. R., de Jeu, R. A., and Dolman, A. J.: Global canopy interception from satellite observations, *J. Geophys. Res. Atmos.*, 115, D16122, doi:10.1029/2009JD013530, 2010.
- Momiyama, H., Kumagai, T. O., Fujime, N., Egusa, T., and Shimizu, T.: Forest canopy interception can reduce flood discharge: Inferences from model assumption analysis, *J. Hydrol.*, 623, 129843, doi:10.1016/j.jhydrol.2023.129843, 2023.
- Montero-Martinez, G., Garcia-Garcia, F., and Arenal-Casas, S.: The change of rainfall kinetic energy content with altitude, *J. Hydrol.*, 584, 124685, doi:10.1016/j.jhydrol.2020.124685, 2020.
- Mostafa, H., Saha, K. K., Tsoulas, N., and Zude-Sasse, M.: Using LiDAR technique and modified Community Land Model for calculating water interception of cherry tree canopy, *Agric. Water Manag.*, 272, 107816, doi:10.1016/j.agwat.2022.
- Mou, J.: Formula for calculating raindrop velocity, *Chin. J. Soil Water Conserv.*, 3, 40–41, 1983.
- Murakami, S.: Water and energy balance of canopy interception as evidence of splash droplet evaporation hypothesis, *Hydrol. Sci. J.*, 66, 1248–1264, doi:10.1080/02626667.2021.1924378, 2021.
- Nanko, K., Mizugaki, S., and Onda, Y.: Estimation of soil splash detachment rates on the forest floor of an unmanaged Japanese cypress plantation based on field measurements of throughfall drop sizes and velocities, *Catena*, 72, 348–360, doi:10.1016/j.catena.2007.07.002, 2008.
- Nanko, K., Onda, Y., Ito, A., and Moriwaki, H.: Effect of canopy thickness and canopy saturation on the amount and kinetic energy of throughfall: An experimental approach, *Geophys. Res. Lett.*, 35, L05402, doi:10.1029/2007GL033010, 2008.
- Nanko, K., Watanabe, A., Hotta, N., and Suzuki, M.: Physical interpretation of the difference in drop size distributions of leaf drips among tree species, *Agric. For. Meteorol.*, 169, 74–84, doi:10.1016/j.agrformet.2012.09.018, 2013.
- Pflug, S., Voortman, B. R., Cornelissen, J. H., and Witte, J. P. M.: The effect of plant size and branch traits on rainfall interception of 10 temperate tree species, *Ecohydrology*, 14, e2349, doi:10.1002/eco.2349, 2021.
- Rutter, A. J., Kershaw, K. A., Robins, P. C., and Morton, A. J.: A predictive model of rainfall interception in forests, 1. Derivation of the model from observations in a plantation of Corsican pine, *Agric. Meteorol.*, 9, 367–384, doi:10.1016/0002-1571(71)90034-3, 1971.
- Senn, J. A., Fassnacht, F. E., Eichel, J., Seitz, S., and Schmidlein, S.: A new concept for estimating the influence of



- vegetation on throughfall kinetic energy using aerial laser scanning, *Earth Surf. Processes Landforms*, 45, 1487–1498, doi:10.1002/esp.4820, 2020.
- Tu, L., Xiong, W., Wang, Y., Yu, P., Liu, Z., Han, X., and Xu, L.: Integrated effects of rainfall regime and canopy structure on interception loss: A comparative modelling analysis for an artificial larch forest, *Ecohydrology*, 14, e2283, doi:10.1002/eco.2283, 2021.
- 370 Valente, F., David, J. S., and Gash, J. H. C.: Modelling interception loss for two sparse eucalypt and pine forests in central Portugal using reformulated Rutter and Gash analytical models, *J. Hydrol.*, 190, 141–162, doi:10.1016/S0022-1694(96)03066-1, 1997.
- Van Dijk, A. I. J. M., Bruijnzeel, L. A., and Rosewell, C. J.: Rainfall intensity–kinetic energy relationships: a critical literature appraisal, *J. Hydrol.*, 261, 1–23, doi:10.1016/S0022-1694(02)00020-3, 2002.
- 375 Wang, S., Liu, C., Li, W., Jia, S., and Yue, H.: Hybrid model for estimating forest canopy heights using fused multimodal spaceborne LiDAR data and optical imagery, *Int. J. Appl. Earth Obs. Geoinf.*, 122, 103431, doi:10.1016/j.jag.2023.103431, 2023.
- Xiao, Q., McPherson, E. G., Ustin, S. L., and Grismer, M. E.: A new approach to modeling tree rainfall interception, *J. Geophys. Res.*, 105, 29173–29188, doi:10.1029/2000JD900343, 2000.
- 380 Yao, W., and Chen, G.: Raindrop falling velocity and terminal velocity formula, *J. Hohai Univ. Nat. Sci. Ed.*, 21, 21–27, 1993.
- Zhang, R., Seki, K., and Wang, L.: Quantifying the contribution of meteorological factors and plant traits to canopy interception under maize cropland, *Agric. Water Manag.*, 279, 108195, doi:10.1016/j.agwat.2023.108195, 2023.
- 385 Zhang, W., Liu, W., Li, W., Zhu, X., Chen, C., Zeng, H., and Yang, B.: Characteristics of throughfall kinetic energy under the banana (*Musa nana* Lour.) canopy: The role of leaf shapes, *Catena*, 197, 104985, doi:10.1016/j.catena.2020.104985, 2021.